Wang et al., https://doi.org/10.1083/jcb.201612123

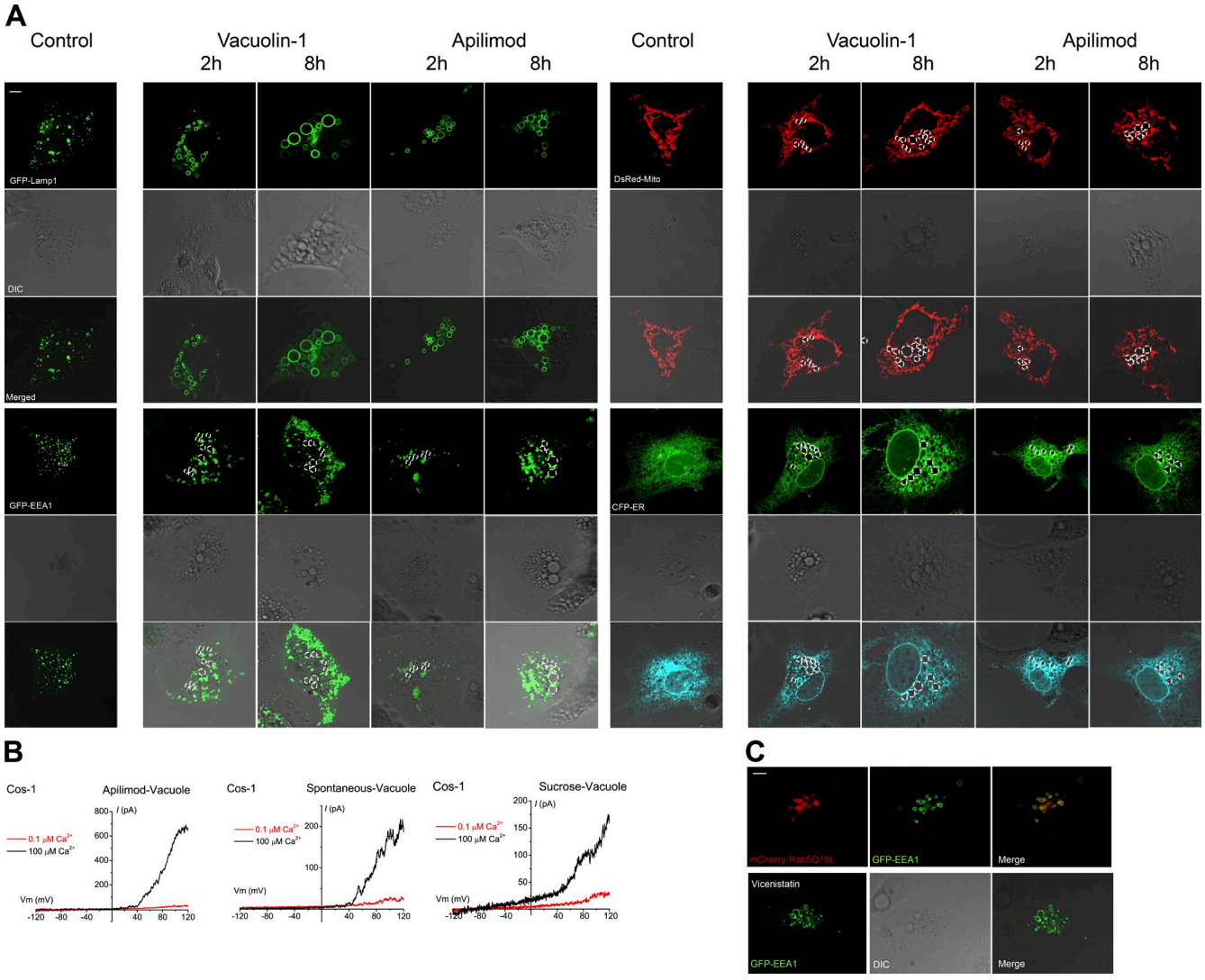

Figure S1. **Vacuolin-1 selectively enlarges endosomes and lysosomes.** (A) Vacuolin-1 and Apilimod (2- and 8-h treatment) enlarged Lamp-1–positive compartments. The enlarged vacuoles were negative for mitochondrial (DsRed-Mito) or ER (CFP-ER) markers. EEA1-positive compartments were slightly enlarged up to 1 µm. Bar, 5 µm. (B) Ca^{2+}-activated outward currents in vacuoles that were enlarged spontaneously, by apilimod (1 µM for 8 h), and by sucrose treatment (50 mM for 8 h), respectively. (C) Overexpressing Rab5-Q79L or application of vicenistatin in Cos-1 cells enlarged EEA1-positive vacuoles. Bar, 10 µm.

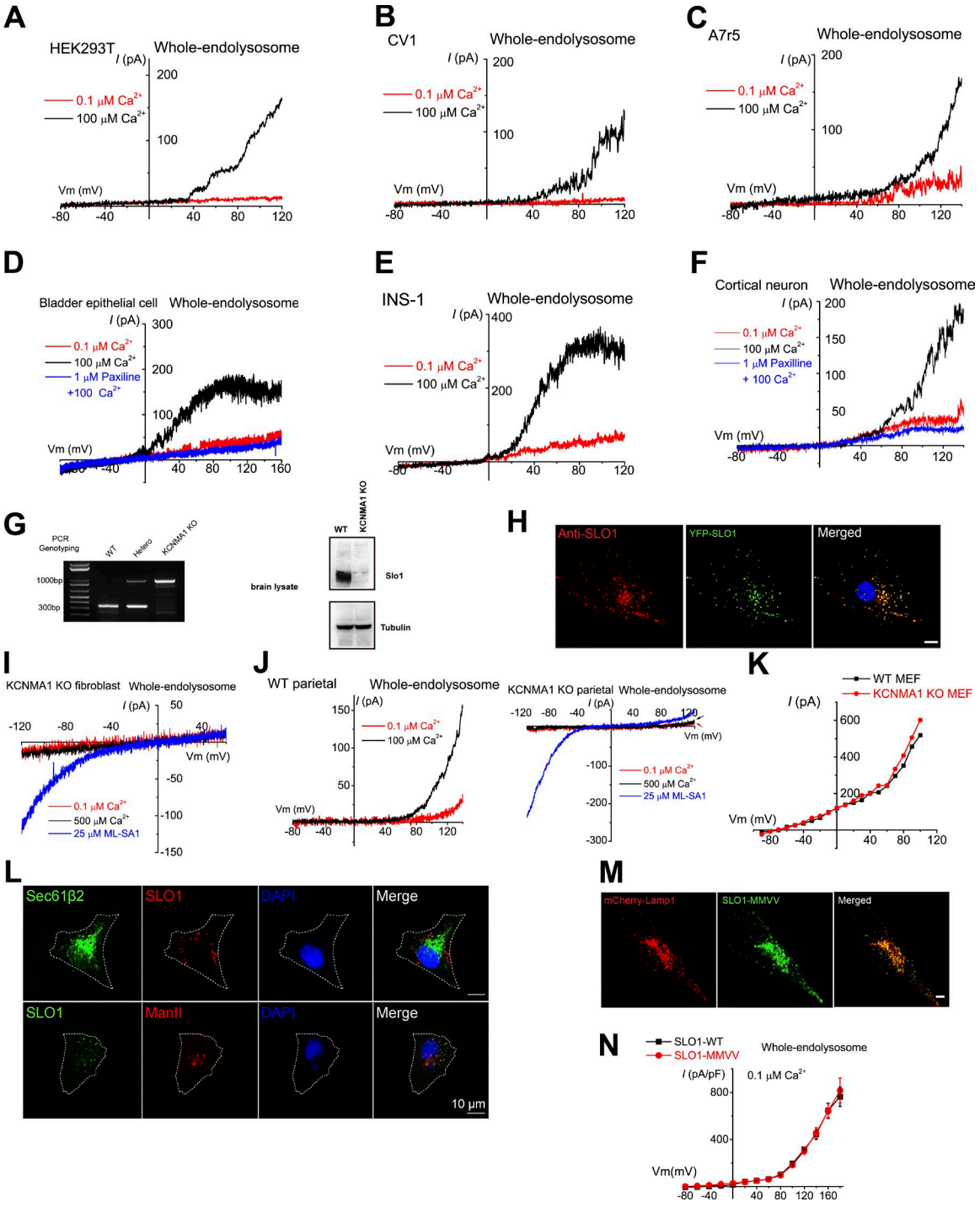

Figure S2. **Lysok$_{VCa}$ currents are present in a variety of cell types.** (A–F) Representative whole-endolysosome Lysok$_{VCa}$ currents in enlarged vacuoles from HEK293T cells (A), monkey kidney CV1 cell lines (B), A7r5 smooth muscle cell lines (C), BECs (D), pancreatic INS-1 cell lines (E), and cultured mouse cortical neurons (F). (G) left, PCR genotyping of WT (*Kcnma1*$^{+/+}$), heterozygous (*Kcnma1*$^{+/-}$), and KCNMA1 KO (*Kcnma1*$^{-/-}$) mice. right, Western blot analysis of endogenous SLO1 proteins using anti-SLO1 antibodies with KCNMA1 KO as controls. (H) Immunofluorescence analysis of overexpressed SLO1 proteins using anti-SLO1 antibodies. Bar, 5 µm. (I) KCNMA1 KO MEFs had whole-endolysosome ML-SA1–activated currents, but no evidence of Lysok$_{VCa}$. (J) Whole-endolysosome Ca^{2+}-activated outward currents in WT and KCNMA1 KO parietal cells. (K) Endogenous whole-cell K^+ currents in both WT and KCNMA1 KO MEF cells. Note that low [Cl^-] (11 mM) was used in the bath solution. (L) Colocalization analyses of SLO1-mCherry with Sec61β2 (an ER marker) and SLO1-GFP with ManII (a Golgi marker). Bar, 10 µm. (M) Confocal images showing the expression of SLO1-MMVV-YFP ($L^{488}I^{489}$ to MM and $L^{734}I^{735}$ to VV) in Cos1 cells. Bar, 10 µM. (N) Lyso-SLO1 currents in cells transfected with WT SLO1-YFP and SLO1-MMVV-YFP.

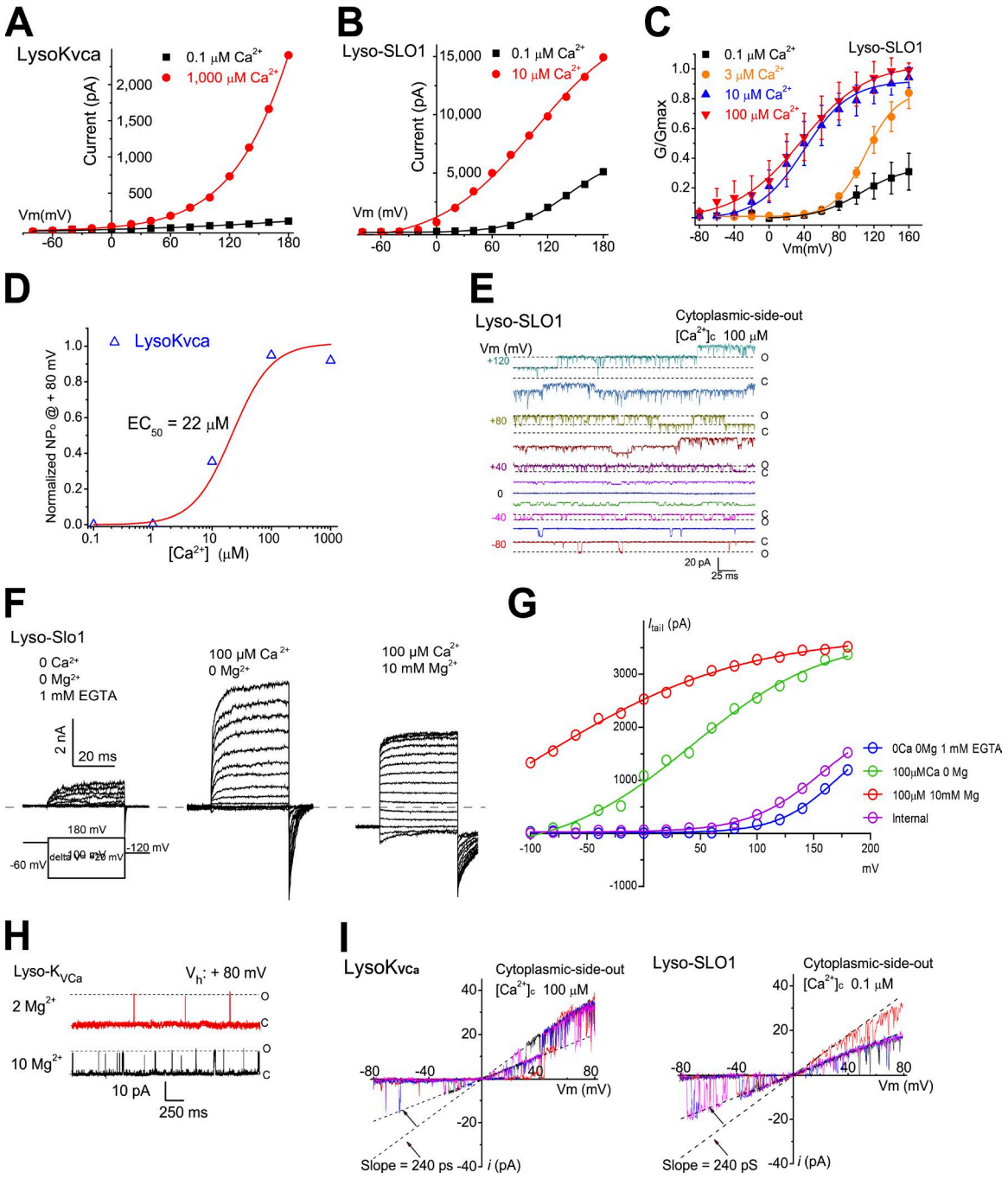

Figure S3. **Regulation of LysoK$_{VCa}$ by Ca^{2+}, Mg^{2+}, and membrane voltages.** (A) Current–voltage relationship (I-V) plot of LysoK$_{VCa}$ based on the step currents shown in Fig. 3 A. (B) I-V of Lyso-SLO1 was plotted based on the step currents shown in Fig. 3 B. (C) Normalized conductance–voltage relationship (G-V) for Lyso-SLO1 at 0.1, 3, 10, and 100 μM $[Ca^{2+}]_C$. The half-maximal activation voltage ($V_{0.5}$; Boltzmann fitting) was shifted from 100 mV at 3 μM Ca^{2+} to 40 mV at 10 μM Ca^{2+}. Error bars indicate SEM. (D) $[Ca^{2+}]_C$ increased NP_o of single LysoK$_{VCa}$ currents with an EC_{50} of 22 μM at 80 mV. (E) Single-channel openings of Lyso-SLO1 across a range of voltages (−80, −40, 0, 40, 80, and 120 mV) from a cytoplasmic-side-out patch at a $[Ca^{2+}]_C$ of 100 μM under symmetric K^+ (cytoplasmic/luminal: 140 mM) solution conditions. (F) Effects of 10 mM $[Mg^{2+}]_C$ and 100 μM $[Ca^{2+}]_C$ on Lyso-SLO1 under symmetric K^+ (140 mM) using a voltage step protocol shown in the bottom left. (G) Tail current analysis of $[Mg^{2+}]_C$ and $[Ca^{2+}]_C$ sensitivities of voltage-dependent activation of Lyso-SLO1 based on the step currents shown in F. (H) Effects of $[Mg^{2+}]_C$ on single LysoK$_{VCa}$ currents at 80 mV. (I) Single-channel currents of LysoK$_{VCa}$ and Lyso-SLO1 generated by voltage ramps from −80 to 80 mV. The slope conductance (dashed lines) was 240 pS for both LysoK$_{VCa}$ (100 μM Ca^{2+}) and Lyso-SLO1 (0.1 μM Ca^{2+}).

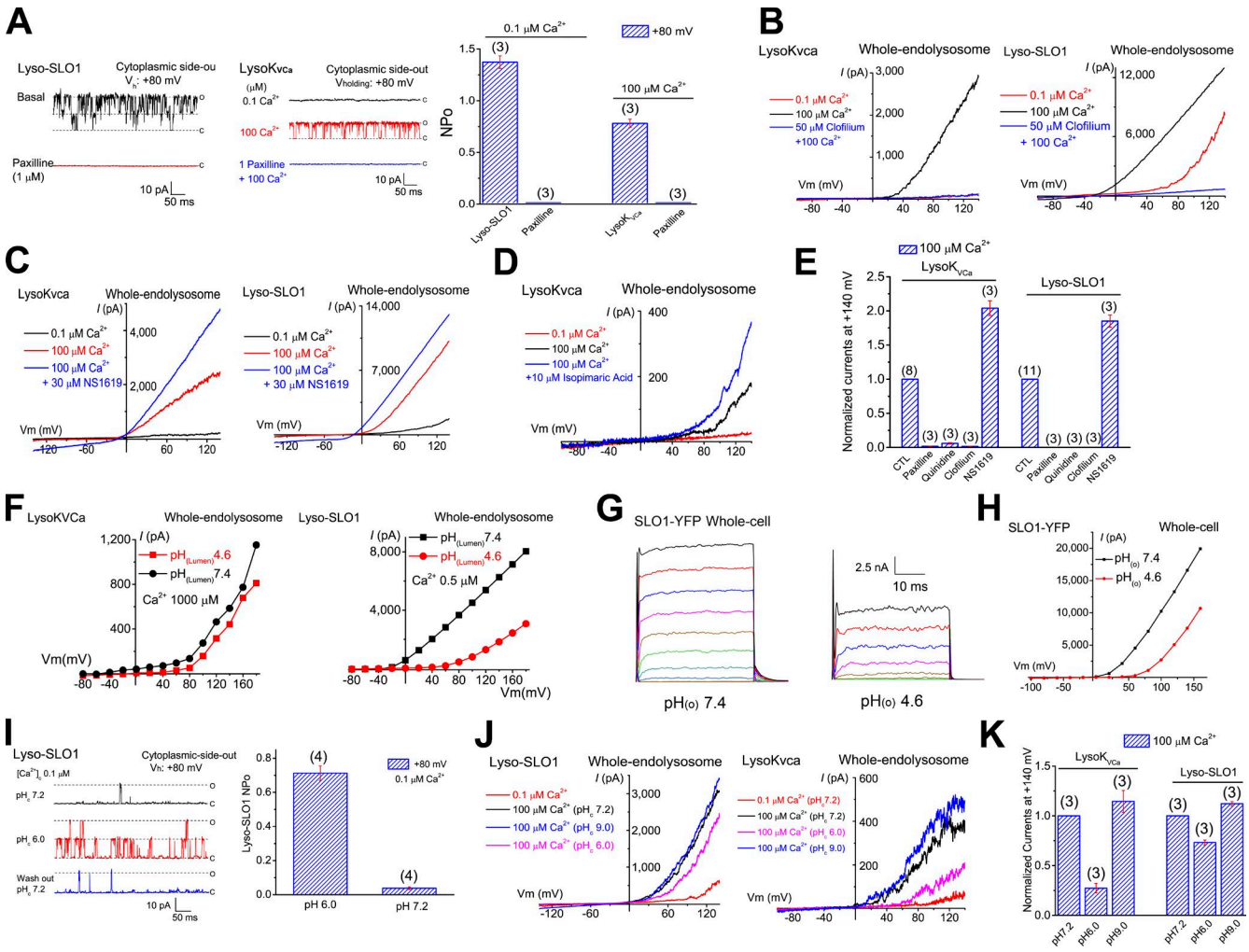

Figure S4. **Regulation of LysoK$_{VCa}$ by BK modulators and pH.** (A) Paxilline (1 µM) inhibited single LysoKvca and Lyso-SLO1 currents completely. (B) Colofilium (50 µM), an inhibitor specific to SLO-family K+ channels, inhibited LysoK$_{VCa}$ (top) and Lyso-SLO1 (bottom) completely. (C) The BK channel opener NS1619 further augmented LysoK$_{VCa}$ and Lyso-SLO1 currents activated by 100 µM Ca^{2+}. (D) Isopimaric acid, another BK channel opener, also potentiated LysoK$_{VCa}$ in the presence of 100 µM Ca^{2+}. (E) Normalized LysoK$_{VCa}$ and Lyso-SLO1 currents at the voltage of 140 mV under different experimental conditions. (F) Representative traces of Lyso-SLO1 activation by 0.5 µM Ca^{2+} under pH$_{(lumen)}$ 7.4 or 4.6. (G and H) Representative step currents showing the effect of acidic extracellular pH (pH$_{(o)}$ 4.6) on whole-cell K^+ currents in SLO1-YFP–expressing HEK293T cells. Currents were elicited by voltage steps from −100 to 160 mV in 20-mV increments with a 100-µM Ca^{2+} pipette solution. Current–voltage relationship of whole-cell SLO1 currents plotted from the step currents shown. (I) Acidic cytoplasmic pH (pH$_c$ 6.0) activated LysoK$_{VCa}$ directly in basal (0.1 µM, calculated based on maxchelator) $[Ca^{2+}]_C$. (J) Alkaline pH$_c$ 9.0 potentiated and acidic pH$_c$ 6.0 inhibited LysoK$_{VCa}$ and Lyso-SLO1 in the presence of 100 µM Ca^{2+}. (K) Normalized LysoK$_{VCa}$ and Lyso-SLO1 currents at the voltage of 140 mV under different experimental conditions. Means ± SEM are shown in A, E, I, and K.

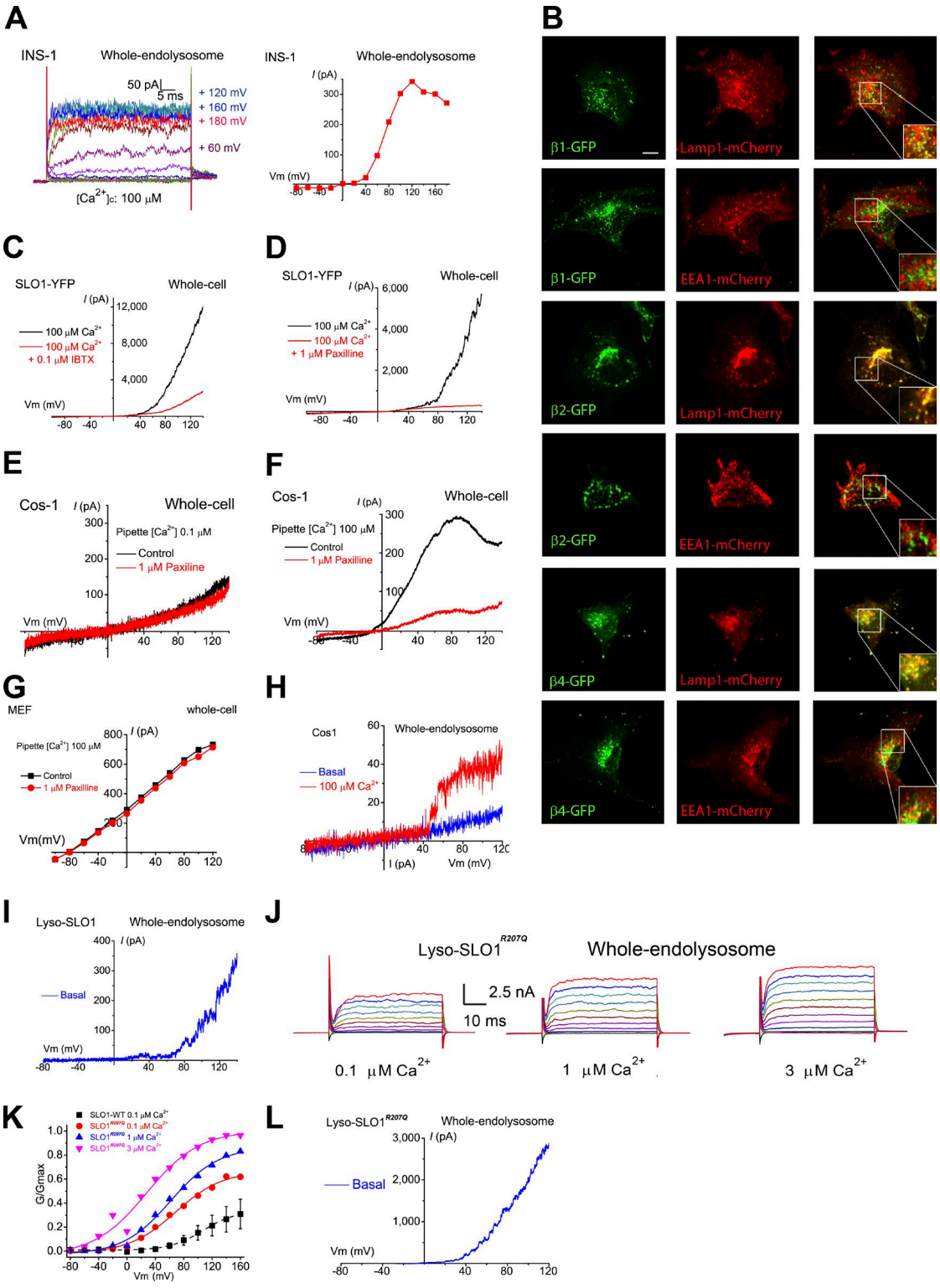

Figure S5. **Cell type–specific properties of Lysok$_{VCa}$ may be conferred by lysosomal localization of auxiliary β subunits.** (A) Representative whole-endolysosome Lysok$_{VCa}$ step currents in INS-1 pancreatic cell lines. The currents were elicited by step voltages from −80 to 180 mV in the presence of 100 μM $[Ca^{2+}]_C$. (B) Colocalization analyses of GFP-tagged KCNMB1 (β1), B2 (β2), and B4 (β4) proteins with Lamp-1 or EEA1 in Cos-1 cells. Note that the colocalization of β2-GFP with Lamp1 was duplicated from Fig. 4 B for comparison. Bar, 10 μM for all images in B. (C and D) Whole-cell K^+ currents were inhibited by bath application of BK inhibitors IBTX (100 nM; C) and paxilline (1 μM; D) in SLO1-expressing HEK293T cells. The pipette solution contained 100 μM Ca^{2+}. (E) Whole-cell K^+ currents in nontransfected Cos-1 cells. The pipette solution contained 0.1 μM Ca^{2+}. (F) Whole-cell K^+ currents were seen in nontransfected Cos-1 cells with the pipette solution containing 100 μM Ca^{2+}. Currents were sensitive to paxilline (1 μM). (G) Whole-cell K^+ currents with or without paxilline (1 μM) application in MEFs. The pipette solution contained 100 μM Ca^{2+}. (H) Activation of Lysok$_{VCa}$ by 100 μM $[Ca^{2+}]_C$ with the same vacuole that was current-clamped in Fig. 5 G. (I) $[Ca^{2+}]_C$ was 0.1 μM. Data are from the same vacuole that was current-clamped in Fig. 5 H. (J) Step currents of Lyso-SLO1^{R207Q} at $[Ca^{2+}]_C$ of 0.1 μM, 1 μM, and 3 μM. (K) Normalized G–V curves of Lyso-SLO1^{R207Q}. Lyso-SLO1 was replotted (dotted line) from Fig. S3 C for comparison. (L) Basal currents of Lyso-SLO1^{R207Q} with 0.1 μM $[Ca^{2+}]_C$. Data are from the same vacuole that was current-clamped in Fig. 5 I.

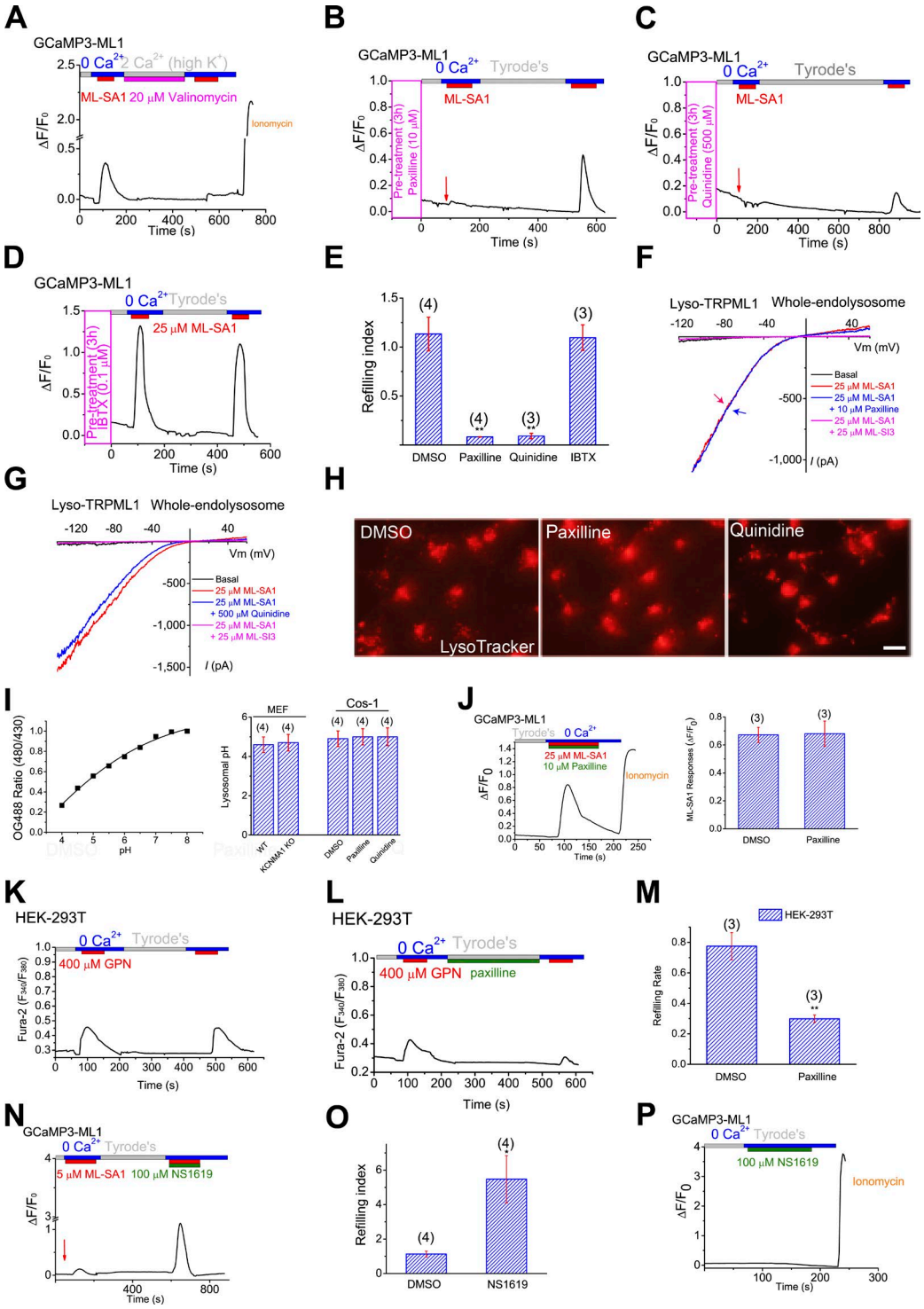

Figure S6. **Regulation of lysosomal Ca^{2+} refilling by $LysoK_{VCa}$.** (A) ML-SA1–induced Ca^{2+} release in HEK-GCaMP3-ML1 cells in the presence of high (140 mM) K^+ extracellular solution. A 5-min valinomycin treatment in the refilling phase abolished lysosomal Ca^{2+} refilling. (B–D) Pretreatment of cells with paxilline (10 µM; B) or quinidine (500 µM; C) for 3 h abolished ML-SA1–induced Ca^{2+} release, whereas IBTX (0.1 µM; D) pretreatment did not affect Ca^{2+}release in HEK-GCaMP3-ML1 cells. (E) Normalized ML-SA1 induced responses in control and paxilline-, quinidine-, and IBTX-pretreated cells. Mean responses of 15–30 cells in one coverslip are shown (mean ± SEM). (F and G) Neither paxilline (F) nor quinidine (G) affected whole-endolysosome ML1 currents, which were activated by ML-SA1 and inhibited by ML-SI3. (H) Pretreatment of Cos-1 cells with paxilline (10 µM) or quinidine (500 µM) for 3 h did not elevate lysosomal pH, which was monitored by LysoTracker (LysoTracker Red DND-99) fluorescence. (I) Lysosomal pH in WT and KCNMA1 KO MEFs and in Cos-1 cells under paxilline and quinidine treatments. (J) Effect of paxilline on naive ML-SA1–induced lysosomal Ca^{2+} release in GCaMP3-ML1 cells. (K–M) Paxilline significantly reduced refill response (second lysosomal Ca^{2+} release) stimulated by GPN in HEK-293T cells. (N) The effects of BK opener NS1619 (100 µM) on lysosomal Ca^{2+} release induced by ML-SA1 in HEK-GCaMP3-ML1 cells. (O) Normalized second ML-SA1 responses to acute application of NS1619. (P) NS1619 did not directly induce lysosomal Ca^{2+} release. Note that this compound is known to induce ER Ca^{2+} release in muscle cells (Wrzosek, 2014). For all panels, means ± SEM are shown. Statistical comparisons were made using variance analysis (Student's *t* test for E, I, J, M, and O). Bar, 50 µm. Statistical comparisons were made with variance analysis (Student's *t* test). *, $P < 0.05$; **, $P < 0.01$.

Reference

Wrzosek, A. 2014. The potassium channel opener NS1619 modulates calcium homeostasis in muscle cells by inhibiting SERCA. *Cell Calcium.* 56:14–24. http://dx.doi.org/10.1016/j.ceca.2014.03.005